

3.1. Introduction

The dielectric materials are very useful in the shrinking of electronic devices and to see this necessity the incorporation and packaging techniques are required. $ACu_3Ti_4O_{12}$ (where $A = Ca, Bi_{2/3}, Gd_{2/3}, Y_{2/3}$) type oxides have a complex Perovskite arrangement and are well known for their capacity to yield high dielectric constants which are required for many critical applications. $ACu_3Ti_4O_{12}$ has high dielectric constant ($\epsilon_r \sim 10^4$) and low loss tangent ($\tan \delta \sim 0.1$) and these types of compounds were discovered in 1967 [Deschanvres *et al.* (1967)]. $BaTiO_3$ is known to be one of the most valuable materials in the family of alkaline earth titanates. Relaxor ferroelectrics such as $Pb(Mg_{1/3}Nb_{2/3})O_3$ [PMN], $Pb(Zn_{1/3}Nb_{2/3})O_3$ [PZN] and $Pb_{1-x}La_x(Zr_{1-y}Ti_y)O_3$ [PLZT] [Moulson, & Herbert *et al.* (2013)] are not environmentally friendly as capacitor materials exhibiting, dielectric constant, $\epsilon_r \sim 1000-20,000$. The problems with $BaTiO_3$ are that it is a ferroelectric Perovskite showing phase transitions with a variation of temperature. The very high dielectric constant ($\epsilon_r \sim 10^4$) value exhibited by $CaCu_3Ti_4O_{12}$ (CCTO) which is nearly constant in the temperature range of 100–600 K, makes it a desirable material for many industrial applications in microelectronics and memory devices. It may extensively be used in the electronic industries for the production of electronic components such as multilayer capacitor, dynamic random access memory, microwave devices, electronic devices in automobiles and aircraft. [Yu *et al.* (2008) Ezhilvalavan & Tseng *et al* (2000), Kretly *et al* (2003), Almeida *et al.* (2004)]. It is established that very fine BTO powders sintering with suitable additives decrease the sintering temperature. However, also, sintering additives can affect the dielectric and electrical properties [Jeon *et al.* (2005), Liu & Roseman *et al.*(1999)]. For example, the accumulation of SiO_2 on BTO decreases the dielectric permittivity of BTO ceramic [Lee *et*

al. (2009)]. CCTO based many composite materials have been studied to improve the dielectric properties using Al₂O₃ [Puchmark & Rujijanagul *et al.* (2012)], TeO₂ [Amaral *et al.* (2011)], GeO₂ [Amaral *et al.* (2010)], Cr₂O₃ [Kwon *et al.* (2008)], SiO₂ [Kim *et al.* (2007)], ZnO [Chen *et al.* (2013)], CaTiO₃ [Fang *et al.* (2006)], SrTiO₃ [Yan *et al.* (2006)] and Ba_{0.6}Sr_{0.4}TiO₃ [Norezan *et al.* (2012)]. The increase in grain boundary resistance or barrier layer in those composites lowers dielectric losses due to the internal barrier layer capacitance. In the present work, composite ceramic of 0.9BaTiO₃ and 0.1CaCu₃Ti₄O₁₂ (BTC) was synthesized by a solid-state method to improve the dielectric properties. This method has the advantages of low processing costs, energy efficiency, and high production rate. The BTC nanocomposite was synthesized by the solid state method and was characterized by XRD, SEM, TEM and AFM techniques. The corresponding dielectric properties were evaluated to understand the best possible properties developed in these composite ceramic.

3.2. Experimental

3.2.1. Synthesis

The composite ceramic of 0.9BaTiO₃–0.1CaCu₃Ti₄O₁₂ (BTC) was manufactured by a modified solid-state route via three steps. Firstly CaCu₃Ti₄O₁₂ (CCTO) was synthesized by semi wet route using analytical grade Ca(NO₃)₂·4H₂O (99.5% Qualigens, India), Cu(NO₃)₂·3H₂O (99.5% Merck, India), Solid TiO₂ (99.5% Merck, India), as the starting materials. In this route, their stoichiometric amounts were mixed in a beaker along with solid TiO₂. Secondly, BaTiO₃ (BTO) was also prepared by a semi wet process using Ba(NO₃)₂ (99% Merck, India), TiO₂ (99.5% Merck, India), and citric acid (99.5% Merck, India) as the starting materials. In this route, their stoichiometric amounts were mixed in a

beaker along with solid TiO₂, and then citric acid (equivalent to metal ions) was added to the solution. The consequential solution was heated on a hot plate with continuous stirring at 70–80 °C to evaporate water and allow for self-ignition. The ignition process was carried out in air, which exhausted a lot of gasses and created a fluffy mass of BTO and CCTO ceramic powders. In this process the mixing of a solution of a metal precursor and an organic poly functional acid having, at least, one hydroxyl group and one carboxylic acid group such as citric, glycine, tartaric or glycerol. Citric acid as a complexing agent can form a complex and provide the fuel for the ignition step. The dry gel of BTO and CCTO were calcined in air at 800 °C for 6 h in an electrical furnace. Thirdly, the amount of the prepared powders of BTO and CCTO by a semi-wet solgel process was mixed. In this process, we used calcined powder of BTO and CCTO as raw materials to synthesize the BTC composite ceramic to develop the modified solid state route to get a nanometer range powders. The mixed BTC nanocomposite ceramic powder was mixed with 2% polyvinyl alcohol (PVA) as a binder and pressed into a cylindrical pellet using a hydraulic press. The PVA binder was burnt out at 500 °C for 5 h. Finally, the BTC nanocomposite pellets were sintered at 950 °C for 3 h, 6 h, 9 h and 12 h respectively.

3.2.2. Characterization

The crystalline phases of BTC nanocomposite sintered samples were identified by using the X-ray diffraction analysis (Rigaku, miniflex600, Japan) employing Cu- α radiation. The microstructures of the fractured surface of sintered ceramics were examined using a scanning electron microscope (Model Quanta 200F, FEI, Nederland) and the particle size was observed using a high-resolution transmission electron microscope (HRTEM, Technai

G2 20 S-Twin). For HRTEM analysis, the specimens were prepared by dispersing the sintered BTC nanocomposite powder in acetone by ultra-sonication. This type of suspensions was deposited onto the carbon coated copper grids. The surface morphology was analyzed by atomic force microscopy [AFM Nano Drive Dimension Edge 8.06 (Build R1MN. 1199088)] the specimens were prepared by dispersing the sintered BTC composite powder in acetone by ultra-sonication, and this type of suspensions was deposited onto the glass slides. The BTC nanocomposite sintered pellets were polished using SiC abrasive paper until they had a surface like a mirror finish. Silver paste was applied to both sides of the circular faces of the ceramic pellets for the purpose of the dielectric and electrical measurements. The dielectric and electrical data of the BTC nano-composite ceramic was obtained using an LCR meter (PSM 1735, NumetriQ 4thLtd, and U.K.) over the frequency range of 100 Hz–5 MHz and in the temperature range of 300–500 K.

3.3. Results and discussion

3.3.1. X-ray diffraction studies

Figure 3.1 shows the XRD pattern of the BTC nanocomposite ceramic sintered at 950 °C for 3 h, 6 h and 9 h and 12 h. It indicates the presence of CCTO and BTO as major phases along with CuO and CaTiO₃ as minor phases (JCPDS – 892475) in the nanocomposite sample sintered for different sintering durations. In the present study, the XRD patterns of the composite ceramic with BTO contents showed the CuO and CaTiO₃ as grain boundary phases which evolve due to the decomposition of the CCTO phase during the sintering process at a different sintering duration. The presence of secondary phases of CuO and

CaTiO₃ was also reported in the glass added CCTO composite at grain boundaries [Norezan *et al.* (2012)].

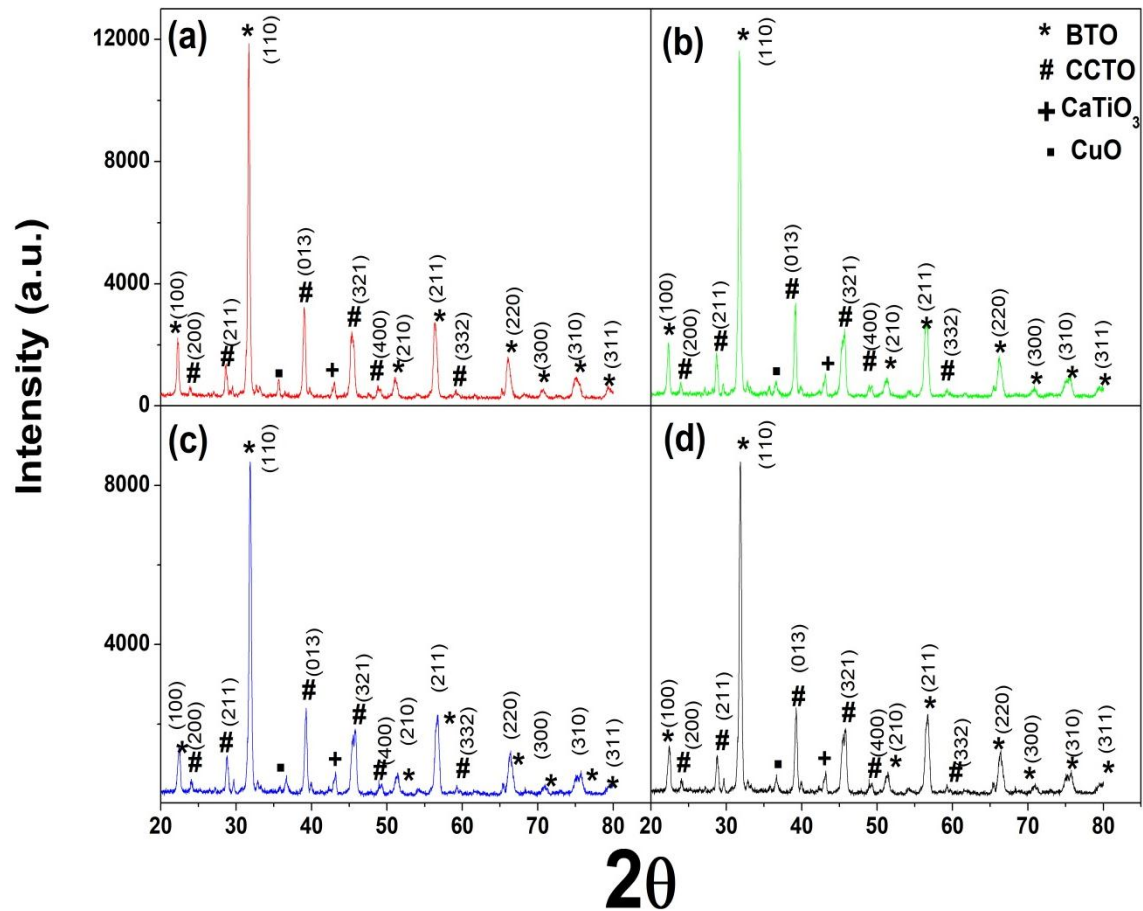


Figure 3.1. X-ray powder diffraction patterns of BTC nanocomposite sintered at 950 °C for (a) 3 h (b) 6 h (c) 9 h and (d) 12 h.

XRD data was also used to determine the average crystallite size (D) of the BTC composite ceramics at different sintering duration using a line broadening method. The Cauchy component of the Voigt function represents the crystallite size, in the single line analysis method; the crystallite size (D) of the BTC nanocomposite at different sintering duration was estimated using the equation 2.2. For the determination of crystallite size of the composite, β values of five most intense XRD peaks lower to higher angles were used in the above mentioned Eq. (2.2). Further to get correct values for crystallite size, line broadening due to instrumental effect (β_i) was removed by using the XRD data for the standard sample. The average crystallite sizes derived from the XRD data were around 21 nm, 24 nm, 25 nm and 26 nm for the BTC ceramic sintered for 3 h, 6 h, 9 h and 12 h respectively.

3.3.2. Microstructural studies

Figure 3.2 shows the bright field TEM image of the BTC nanocomposite sintered at 950 °C for 12 h. The image of the ceramic reveals the presence of nanoparticle in the size range of 30 ± 10 nm. The TEM observation suggests that the ceramic powder synthesized in this system is close to the nanocrystalline in nature. The particle sizes observed by TEM were approximately close to the average crystallite size determined from the XRD data.

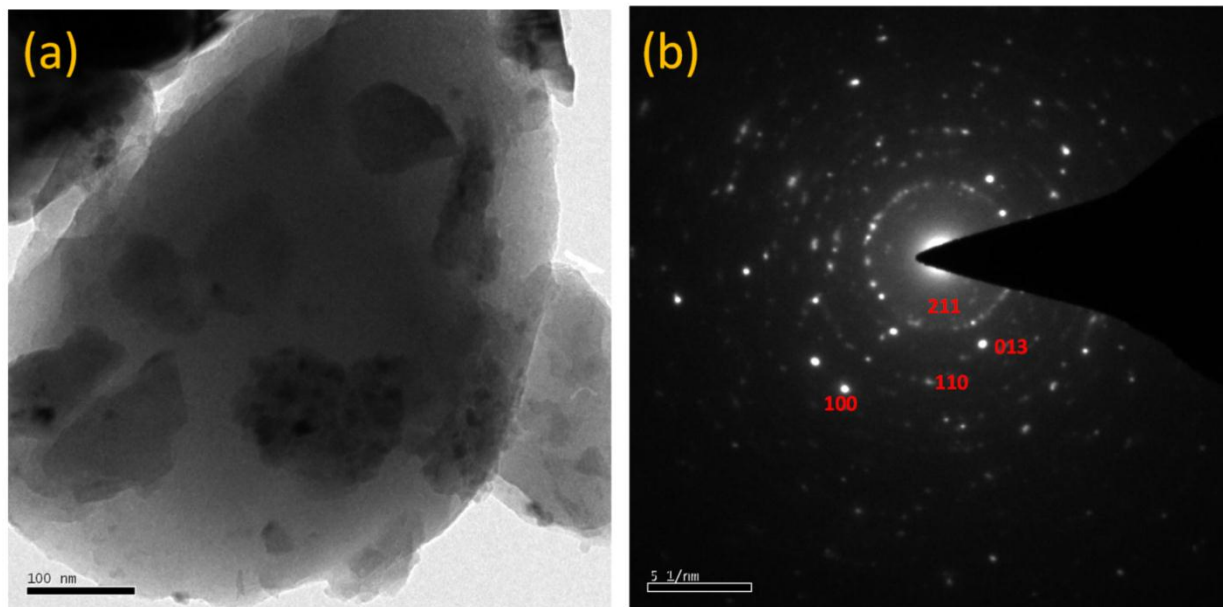


Figure 3.2. (a) Bright field TEM images and (b) SEAD pattern of BTC nanocomposite sintered at 950 °C for 12 h.

The SEM image of the BTC nanocomposite sintered at 950 °C for different time duration is shown in Figure 3.3. The grain size ranges of the BTC nanocomposite are 269 nm, 309 nm, 342 nm, and 734 nm sintering for 3 h, 6 h, 9 h and 12 h respectively. The morphology of the BTC nanocomposite ceramic shows the exclusive topographies with the bimodal spherical grains. The smaller grains are in nanometer whereas other larger in micrometres ranges [Kim *et al.* (2013)].

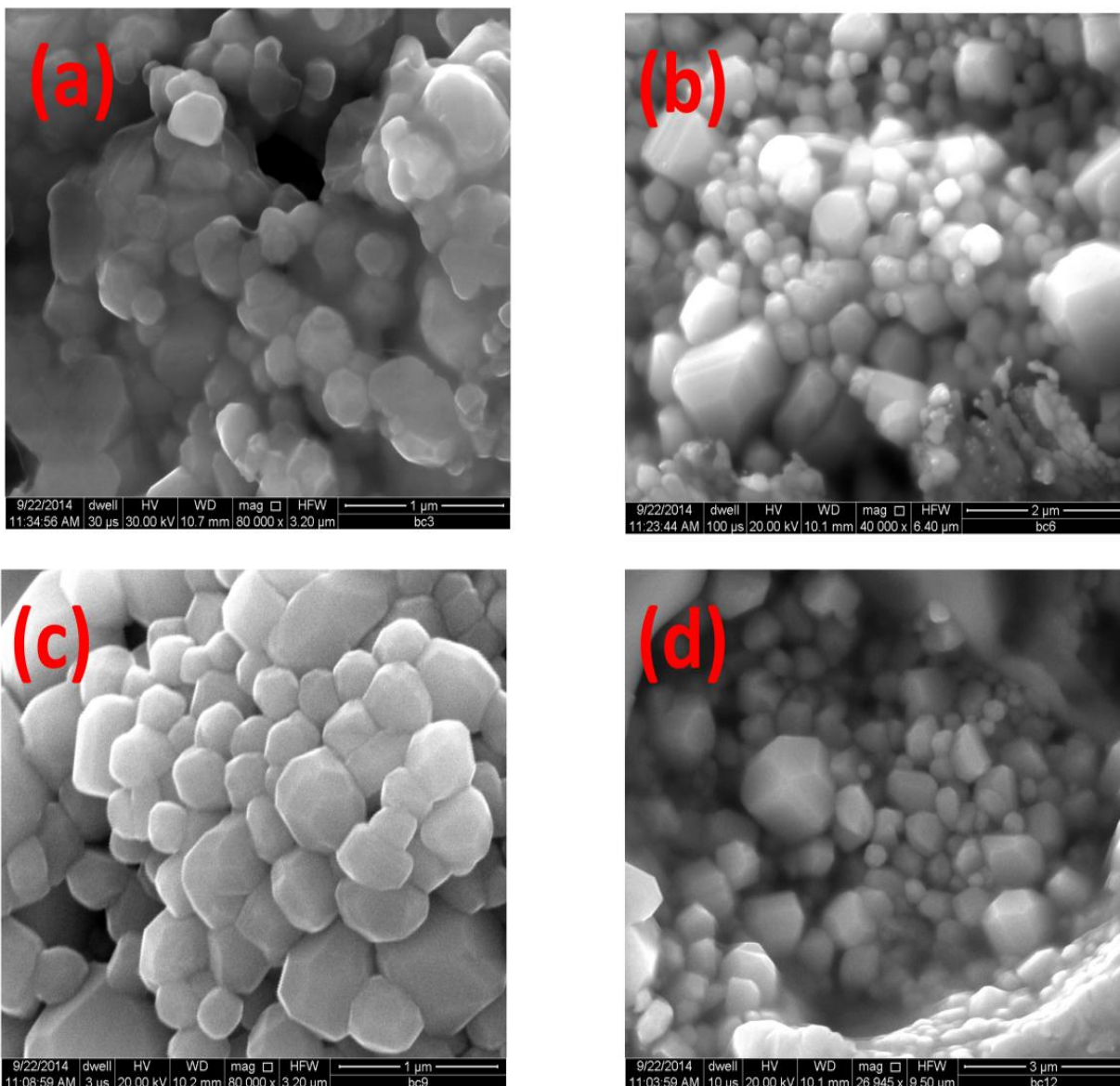


Figure 3.3. SEM micrographs of BTC nanocomposite sintered at 950 °C for (a) 3 h (b) 6 h (c) 9 h and (d) 12 h.

The AFM images are shown in Figure 4(a) and (b) of the BTC nanocomposite pellet sintered at 950 °C for 12 h which indicates that the bimodal nature of BTC nanocomposite. The average roughness and root mean square (RMS) data were obtained as 3.64 nm and 5.55 nm respectively on scanned area 1 μm × 1 μm where ten different points were used for the calculation of mean value. Figure 4(c) shows the histogram of particle roughness and Figure 4(d) shows the histogram of particle sizes of BTC composite ceramic recorded by AFM using tapping mode.

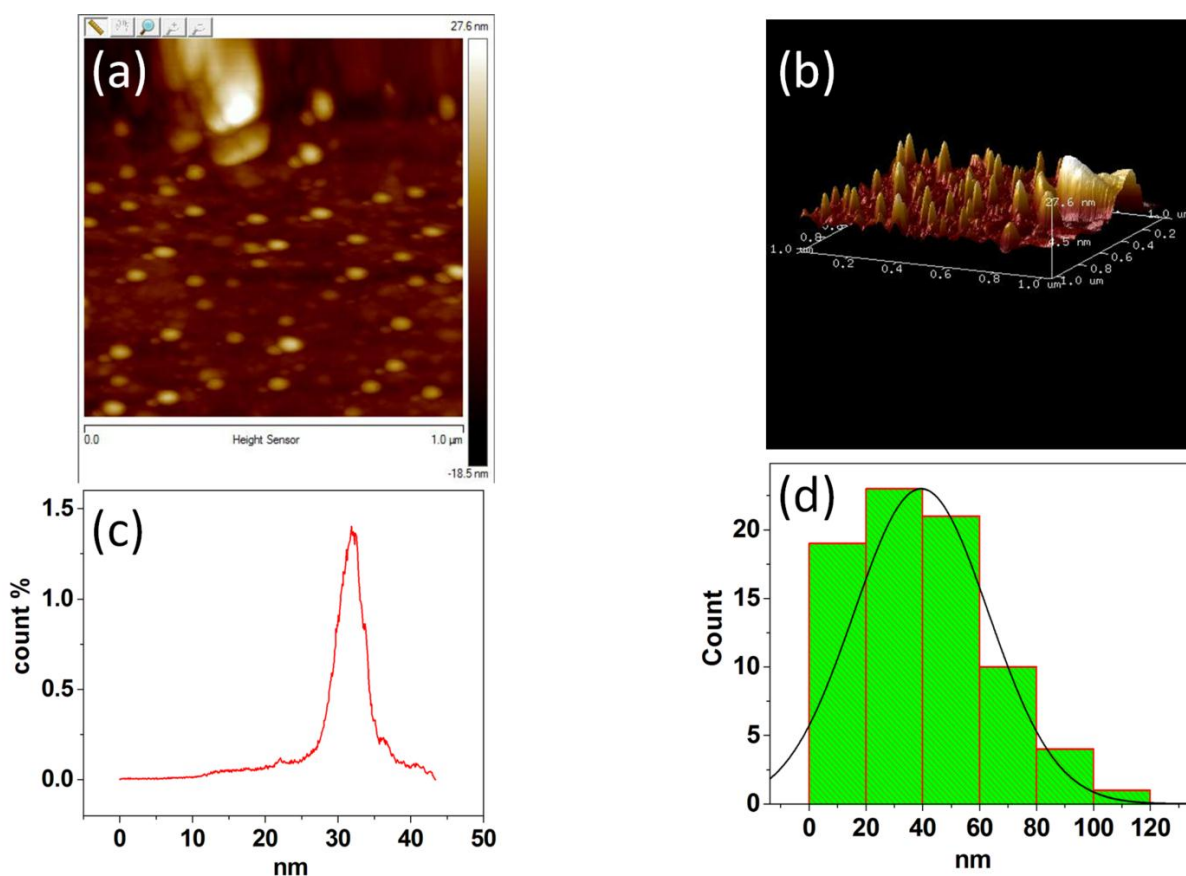


Figure 3.4. AFM images of BTC nanocomposite sintered at 950 °C for 12 h (a) 2 dimensional (b) 3D structure (c) depth histogram (d) bar diagram of particles size.

It is observed from the figure that the most of the particles are in a range of 20 nm to 40 nm. The average size and area of particles were found to be 30 ± 10 nm and 1326 nm^2 respectively. The particle sizes observed by AFM are in agreement with the results determined by TEM and XRD.

3.3.3. Dielectric studies

Figure 3.5 shows the variation of the dielectric constant and the dielectric loss with a change of temperature at 1 kHz for the BTC nanocomposite at few selected sintering durations. It is observed from the Figure 3.5(a) that the composite sintered for 3 h shows a dielectric constant peak in the temperature range of 300–380 K, and then the value seems to be constant up to the measured temperature of 500 K. The composite is sintered for 6 h, 9 h, and 12 h show constant values of dielectric constant in the temperature range 300–500 K. From the figure it is also observed that the dielectric constant decreases with the increasing sintering duration. The absence of peak for composite sintered for high sintering period confirm the composite formation. We can thus conclude that 3 h sintering duration is insufficient for BTC nanocomposite structure. The dielectric constant of the composite was found to be 1713, 731 and 110 sintered at 950 °C for 6 h, 9 h, and 12 h respectively and at 1 kHz. The value of dielectric constant of the BTC nanocomposite is high due to the existence of large semiconducting grains and the presence of the insulating grain boundaries. The presence of the internal barrier layer capacitance (IBLC) supporting the appliance responsible for the high value of dielectric constant existing in this composite ceramic [Kai *et al.* (2004)].

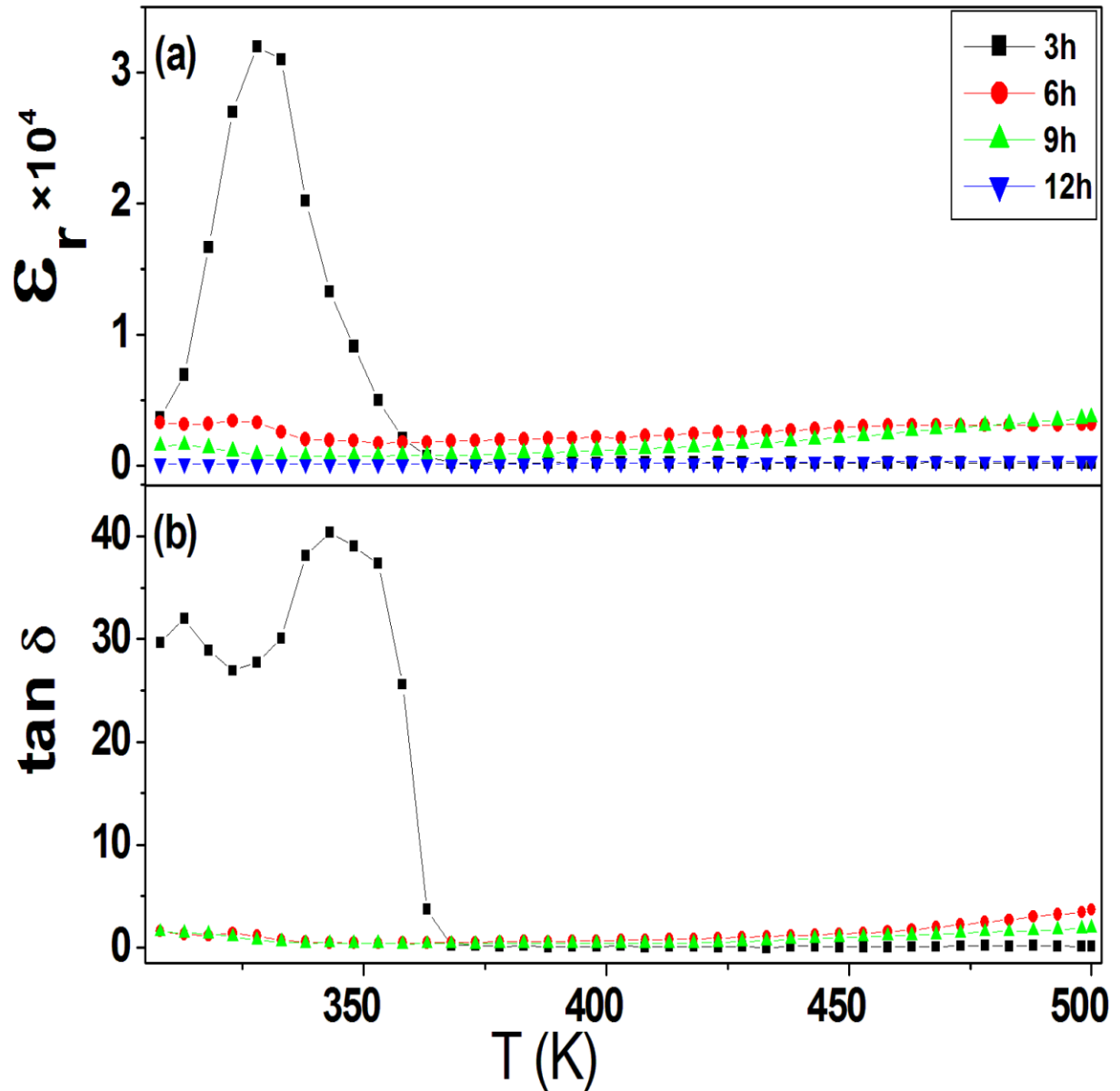


Figure 3.5. (a) Plots of the dielectric constant (ϵ_r) versus temperature and (b) $\tan \delta$ versus temperature at 1 kHz for sintered at 950 °C for 3 h, 6 h, 9 h, and 12 h.

The dielectric loss peaks are also observed for the composite sintered at 950 °C for 3 h in the temperature range of 300–380 K (Figure 3.5(b)) and their dielectric loss is nearly constant up to the temperature of 500 K. The value dielectric loss was found to be 0.443, 0.410 and 0.156 for the composite sintered for 6 h, 9 h and 12 h, respectively at 350 K and 1 kHz. The value of $\tan \delta$ increase rapidly at higher temperature due to increasing of a conductivity of the composite with temperature as is usually observed [Prakash & Varma *et al.* (2007), Chen *et al.* (2004)]

Figure 3.6 shows the variation of dielectric constant and dielectric loss with frequency at 50 °C for the composite sintered at 950 °C for 3 h, 6 h, 9 h and 12 h. It is observed from the Figure 3.6(a) that the dielectric constant decreases with increasing frequency. The value of dielectric constant at 50 °C and 1 kHz was found to be 3.2×10^5 , 9.5×10^3 , 1.3×10^3 and 1.2×10^2 for the BTC nanocomposite sintered for 3 h, 6 h, 9 h and 12 h respectively. The inset figure shows the dielectric constant variation at higher frequency region which clearly shows different values of dielectric constant. It can be seen that the value of the dielectric constant of the composite sintered for 3 h is higher than the value of other sintered samples. It is also observed that the dielectric constant decreases with increasing frequency and then remains constant at high frequency region which may be explained due to the periodic reversal of the field takes place so rapidly that there is no charge accumulation at the interface, resulting in a constant ϵ_r value.

Figure 3.6(b) shows the dielectric loss peak for the composite sintered for 3 h clearly and also for the composites sintered for 6 h, 9 h, and 12 h, as shown in the inset figure. The presence of the dielectric loss peaks in the composites confirms the presence of dielectric relaxation in the composite. When two phases of grain, grain-boundaries of different

electrical conductivities were in contact, then the low-frequency relaxation may be due to the resulting space charge polarization [J.L. Zhang *et al.* (2005), P.R. Bueno *et al.* (2007)].

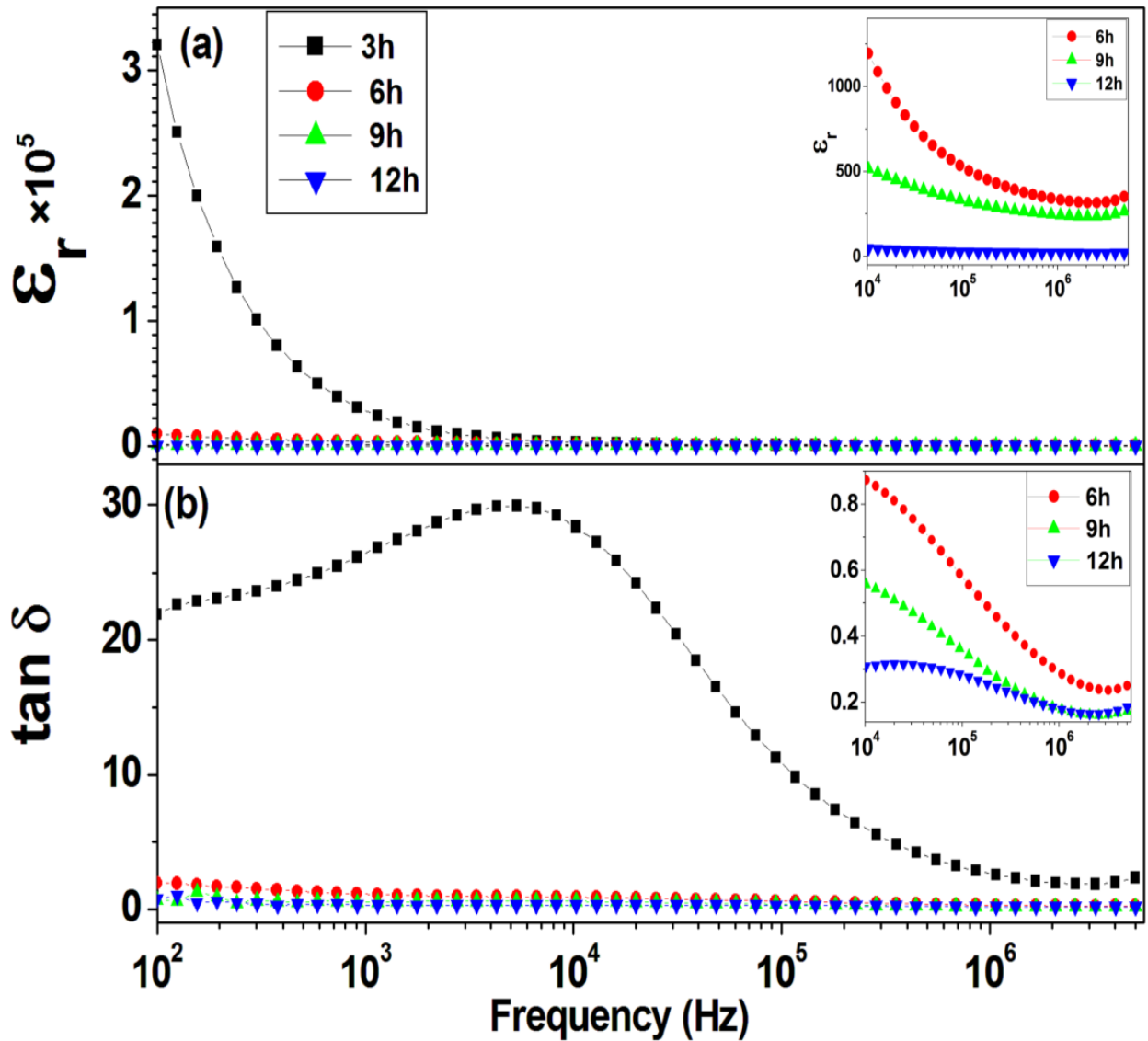


Figure 3.6. (a) Plots of the dielectric constant (ϵ_r) versus frequency and (b) $\tan \delta$ versus frequency at 50 °C for BTC nanocomposite sintered at 950 °C for 3 h, 6 h, 9 h and 12 h.

3.3.4. Conductivity studies

The dependence of AC conductivity on the frequency at 50 °C for the BTC composite sintered for 3, 6, 9 and 12 h time duration showed in Figure 3.7. The conductivity of the composite sintered for 3 h is remains constant up to 1 kHz which gives the DC value of conductivity (σ_{dc}). The value of σ_{dc} was found to be $3.9 \times 10^4 \Omega^{-1} \text{ cm}^{-1}$. The composite sintered for 6 h, 9 h, and 12 h show continuous variation in conductivity from lower to higher frequency regions at 50 °C. The variation of conductivity with frequency may be explained by the following equations;

$$\sigma_{\text{total}} = \sigma_{\text{ac}} + \sigma_{\text{dc}} \quad (3.2)$$

$$\sigma_{\text{ac}} = A\omega^s \quad (3.3)$$

The frequency independent part of conductivity is the DC conductivity (σ_{dc}). A is a temperature dependent constant which controls the magnitude of dispersion at different sintering duration, and s is constant known as exponents. The value of s was found to be 0.73, 0.70, 0.68 and 0.66 for sintering duration 3 h, 6 h, 9 h and 12 h respectively. The value of exponents (s) signifies the degree of interactions of mobile ions. The exponents values greater than zero and less than one ($0 \leq s \leq 1$) characterizes the low-frequency region, corresponding to translational ion hopping [S. Mollah *et al.* (1992)].

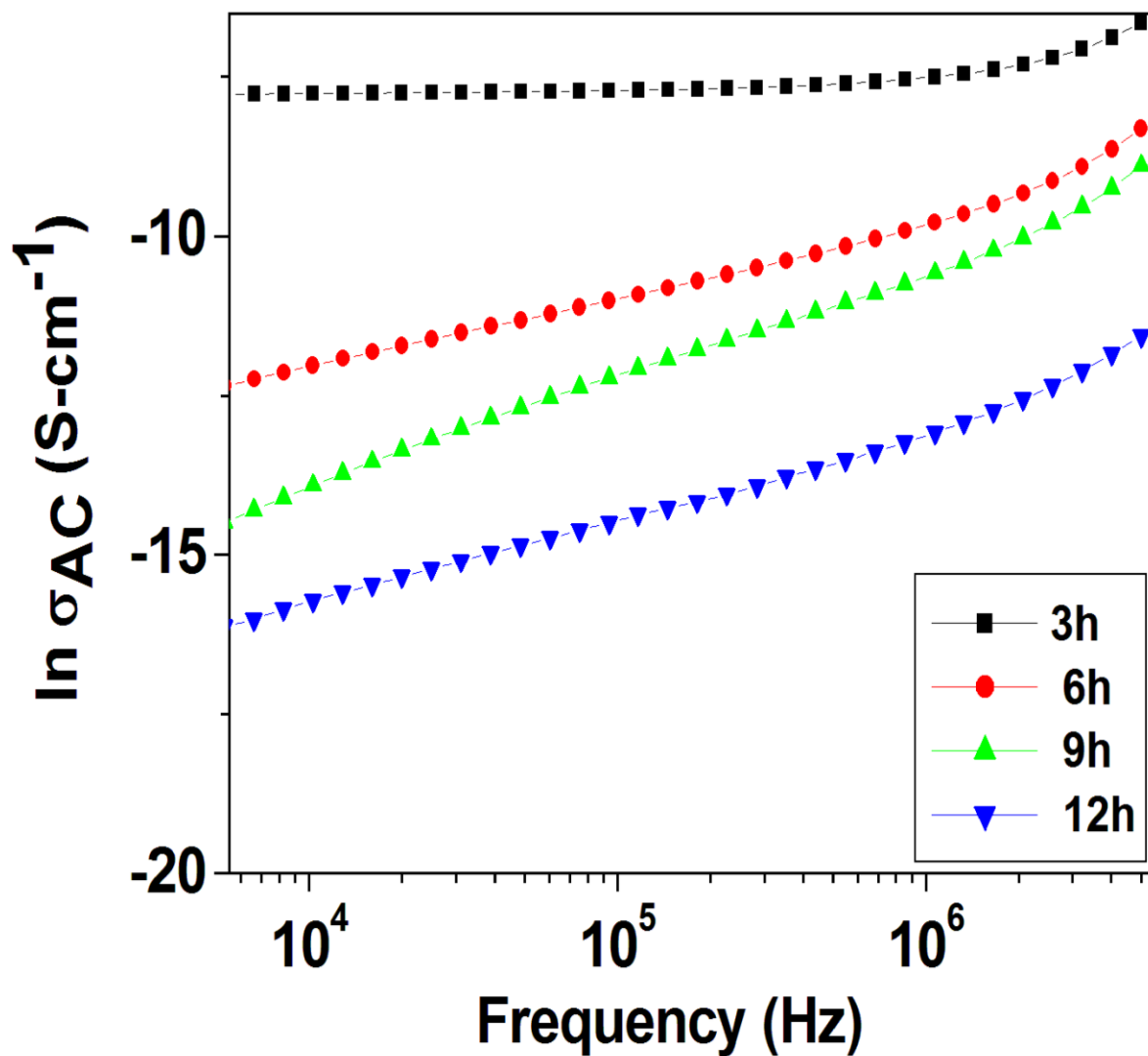


Figure 3.7. Plot of the AC conductivity vs. frequency at a temperature of 50 °C for BTC nanocomposite sintered at 950 °C for 3 h, 6 h, 9 h and 12 h.

3.4. Conclusion

In this work we report the synthesis of BTC nanocomposite through a modified solid state route by sintering at 950 °C for 3 h, 6 h, 9 h and 12 h. The average particle size of the BTC nanocomposite sintered for 12 h is 30 ± 10 nm obtained by TEM and XRD analysis. The scanning electron microscopy analysis shows the presence of bimodal behavior of grains. The microstructural analysis shows the grain growth of BTO was largely affected by CCTO. The average and RMS roughness of the BTC nanocomposite were studied by atomic force microscope (AFM) using tapping mode of measurement. The value of dielectric constant of the BTC nanocomposite sintered for 3 h is higher than that of 6, 9 and 12 h at 1 kHz and low dielectric loss at higher duration. The conductivity of the BTC nanocomposite sintered for 3 h is greater than that of the BTC nanocomposite sintered for 6, 9 and 12 h which is responsible for the high dielectric constant of this ceramics.